Analysis of piles-anchor supporting marine walls

Mohamed E. El-Naggar
Civil Eng. Dept., Faculty of Eng., Alexandria University, Alexandria, Egypt

This paper presents the analysis of laterally loaded piles which are used to support the anchors for bulkheads walls. The problem has been examined by plain-strain non-linear finite element analysis. The soil has been modeled as elasto-plastic medium. Fifteen nodes element has been employed to model both the soil and the anchored bulkhead elements. The pile has been modeled as five nodes beam element. Parametric study has been produced in order to investigate the lateral displacements, the shearing forces and the bending moments along the pile shaft. The ultimate tie force, which the system can carry, has been also investigated. Based on the finite element analysis, the load carrying capacity of the anchored-block pile system is significantly increased with the increase of both the width and the thickness of the anchored-block pile head. The pile length, pile diameter, spacing between piles, soil stiffness, angle of internal friction, and soil unit weight have also greatly affected the behavior of the anchored-block pile system. Based on the analysis, design equations to investigate the ultimate load, the maximum lateral displacement of pile-head, the maximum shearing force and the maximum bending moment in the pile shaft are presented.

الغرض من هذا البحث هو دراسة وتحليل الخوازيق الرأسية المستخدمة في تثبيت المرابط الخلفية لحوائط الأرصفة وتحديد العوامل المختلفة التي قد تؤثر علي تصميم ذلك النوع من المنشآت البحرية وذلك بهدف زيادة اتزانها وتقليل الإزاحات الأفقية عند رأس الخازوق وتحديد القوي الداخلية المؤثرة علي الخوازيق وكذلك أقصي شد علي المرابط الخلفية. ولتحديد تأثير العوامل المختلفة والمؤثرة علي اتزان هذا النوع من المنشآت فقد تم استخدام نظرية العناصر المحددة لدراسة كل عامل علي حده ومن ثم تحديد تأثير كل العوامل مجتمعة. وقد أوضحت الدراسة انه كلما زادت جساءة المربط الخلفي وكذلك طول الخازوق وجساءة التربة المحيطة بالخوازيق كلما قلت الحركة الأفقية عند رأس الخازوق والعزوم الداخلية المتولدة في الخازوق وزادت قوة تحمل المنشاء لمقاومة قوي الشد المتولدة في المرابط الخلفية وقد تم استنتاج معادلات نظرية لتحديد أقصي حركة أفقية متولدة عند رأس الخازوق و أقصي قوة قص وأقصي عزم متولدة علي طول الخازوق وكذلك أقصي قوة شد يتحملها المنشاء نتيجة لتأثير جميع العوامل المؤثرة علي أتزان هذا النوع من المنشآت.

Keywords: Anchored-block, Bulkheads, Lateral displacement, Laterally loaded pile, Port design

1. Introduction

Piles are structural members used to carry the superstructure loads through the soil. Early designers assumed piles could carry only vertically axial loads, but piles are often subjected to both vertical and lateral loads. Anchors for bulkheads, fender dolphins, waterfront and offshore piles subjected to wave forces and many marine piling represent a large class of piles subjected to lateral loads.

The response of a pile to lateral loads is a typical example of the classical soil-structure interaction. Several analytical methods have been proposed to predict the response of laterally loaded piles. Finite difference is the early method used. Bowles [1] mentioned that Matlock and Reese used this method to obtain a series of non-dimensional curves to estimate the ground-line deflection and maximum bending moment in the pile shaft. The results limited the parametric study which may be essential in making the most economical solution.

The p-y analysis is a well-known method used in analyzing the non-linear load-deflection behavior of the laterally loaded piles [2-7]. It was based on the beam-on-elastic foundation analysis. In this method, the soil surrounding the pile is simulated by a series of independent non-linear springs; each spring represents the behavior of a soil layer of unit width. To derive the load-deformation characteristics of piles, an appropriate sub-grade reaction modulus must be chosen to represent the combination of the pile and the surround-

ing soil. Unfortunately, the sub-grade reaction modulus is usually estimated by empirical correlations that may lead to uncertainties and inaccurate solutions. Furthermore, the p-y ignored the continuum nature of the soil.

Elastic-plastic solution has been used also in the analysis of laterally piles. It was developed for a free-head pile [8] and a fixed-head pile [9,10]. In this method, the pile-soil response has been simulated as a series of independent springs acting along the pile shaft and the pile base.

Full-scale field tests have been also used to investigate the behavior of laterally load piles. Alizadeh et al. [11] and Mokwa et al. [12] provided considerable results to represent the response of piles based on field tests.

Based on the previous approaches, it has been found that there is a need for understanding the nonlinear behavior of pile under lateral load especially when it used to support the anchor bulkhead. In the present study, nonlinear finite element analysis has been employed to study the behavior of single pile fixed with an anchor bulkhead. Lateral displacements, shearing forces and bending moments induced along the pile shaft have been calculated due to the effect of different system parameters. Furthermore, the ultimate load carried by the system has been also investigated.

2. Geometry of the structure

Fig. 1 illustrates the geometry of anchor-block-pile system considered for this work. It has been found from the previous approaches that the extension of the surrounding soil from the center of the pile should be greater than or equal thirty times the pile diameter, D, and the depth of soil below the pile tip should be greater than or equal forty times the pile diameter Maharaj, D. K. [13].

In the numerical analysis, the pile was considered as a linear elastic member that can interact with the anchor-block and the surrounding soil. The anchor-block was treated as a linear elastic plate supported by the underneath pile. Since Mohr-Coulomb failure criterion is currently the most widely method used for soil in practical applications, the soil was presented as elastic-perfectly plastic material based on Mohr-Coulomb failure criterion.

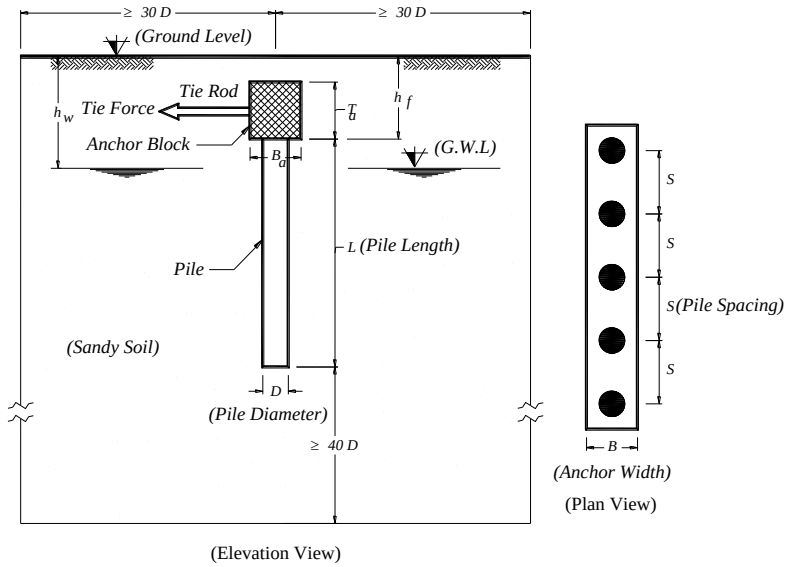

Fig. 1. Geometry of anchor-piles system.

Plain-strain nonlinear analysis, through the finite element program PLAXIS [14] has been used to study the interaction between anchor-block, pile and soil under lateral load.

All the nodes on the lateral boundaries are restrained from moving in the horizontal direction to represent the rigid-smooth lateral boundaries. And to represent the rough-rigid surface boundaries, all the nodes on the bottom surface are restrained in both horizontal and normal directions. 15-node triangle elements have been used to model both soil and anchor-block elements. It is a very accurate 2-D element which has been shown to produce high quality stress results for difficult problems and perform well for most types of calculation, [15,16]. 5-node beam elements have been used to model pile elements. The interface between the pile and the surrounding soil was modeled using 5-node interface elements of zero thickness. The finite element mesh was refining greatly around the pile and the anchor-block to account the behavior of the anchor-block-pile system. Fig. 2 presents the schematic 2-D finite element mesh used for the present work.

Series of 2-D plain strain finite element models were performed on anchor-block supported by five piles in the transverse direction. The analysis were performed with different lengths, diameters and spacing in transverse direction of pile; different modulus of elasticity and angle of internal friction of soil, and different widths and thicknesses of anchor-block. The results obtained from the finite element model was verified and sub-stantiated by the results on the field tested models.

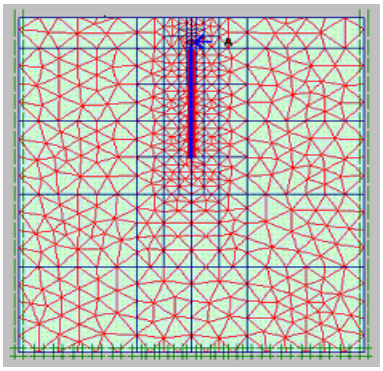

Fig. 2. Finite element model as generated by PLAXIS.

3. Plain strain finite element model for piles

The interaction of anchor-block, pile and soil is very complex to model in any theoretical analysis. To overcome this complication, plain strain analysis has been used [17, 18]. The piles are simplified into strips with equivalent pile Young's modulus, E_{eq}, given by Prakosa and Kulhawy [18] as:

$$E_{eq} = \frac{N_i . A_p E_p}{L_a . D} . \quad (1)$$

In which; N_i is the number of piles in row *(i)*, A_p is the area of pile cross section, E_p is the Young's modulus of pile material, L_a is the length of anchor block (in plan), and D is pile diameter.

To simulate the side shear resistance of the actual piles in plain strain finite element model, the side shear resistance of the equivalent plain strain piles should be equal the side shear resistance of the actual row of piles. Prakosa et al. [18] mentioned that plain strain pile has two sides, the equivalent side shear resistance for the interface element at a given depth on each side, f_{eq}, is given by the following equation:

$$f_{eq} = \frac{N_i . A_s f_s}{2 L_a} . \quad (2)$$

In which; A_s is the surface area of pile per unit length and f_s is the side shear resistance of pile per unit length.

Prakosa et al. [18] did not suggest any modification for the pile tip resistance. PLAXIS finite element program was used throughout this work to analyze vertical piles which are used to support the anchored block of bulkhead walls.

4. Material properties

The soil adopted in this work was assumed to be homogenous sand and has the following properties: modulus of elasticity, E_s, varies from 20 MPa to 80 MPa; Poisson's ratio, ν_s = *0.30*; its dry unit weight γ_{sd}, varies from *15* to *20* kN/m^3 and its angle of internal friction, ϕ, varies from 25^o to 40^o. The concrete piles used herein have the following properties: modulus of elasticity, E_p = *20 GPa*; Poisson's

ratio, ν_p = *0.20* and its dry unit weight γ_d = 25 kN/m^3. The anchor-block has the same quality as the piles.

5. Results and discussions

It has been found from the parametric studies that all the parameters pertaining to the anchor-block pile system have a significant effect on the behavior of the structure. To represent this effect, the results obtained from the anchor-block height ratio, T_a/D parameter was considered as an example of the analysis in the following subsections.

5.1. Load deflection behavior

Fig. 3 represents the load-displacement relationship for anchored-block-pile system of different anchored-block thickness ratio, T_a/D till failure, in which T_a is the thickness of anchored-block and D is the pile diameter. The structure was examined due to low and high stiffness of the anchored-block. The results show that when the stiffness of the anchored-block increases the load carrying capacity of the structure increases. It increases by about 40 and 82% as the T_a/D ratio changed from 1 to 3 and 5, respectively. As well as, for a specified load, the lateral displacement decreases with the increase of T_a/D ratio. For example, at a lateral load of *400 kN/m*, the lateral displacement ratio, Δ/L was reduced by nearly 24 and 35% as the T_a/D ratio changed from 1 to 3 and 5, respectively, where Δ is the lateral displacement and L is the pile length.

All types of piles show nearly the same behavior under the low level of loading, soil in elastic state, beyond this level the behavior is totally different, soil in plastic state. Piles of small height ratio reached to its ultimate lateral load carrying capacity first followed by the greatest height ratio piles. This behavior occurred due to the contribution of passive earth pressure developed over the anchor-block height since the increase of anchored-block height leads to increase the passive earth pressure affected over this height and then reduces the lateral displacements and increases the load carrying capacity of the structure.

Fig. 4 presents the effect of anchored-block height ratio, T_a/D on the lateral displacement ratio, Δ/L along the pile length. The analysis was carried till the structure failed. The results show a significant reduction in the maximum lateral displacement due to the increase of T_a/D ratio. The reduction was about 54 and 78% as the T_a/D ratio increased from 1 to 3 and 5, respectively. This reduction could be expected as a result of the contribution of passive earth pressure to increase the lateral load carrying capacity as mentioned above.

It can be also seen that the lateral response of piles is nonlinear. It is different along the pile shaft. The maximum lateral displacement happened at the pile head and then reduced till approximately zero at the pile tip.

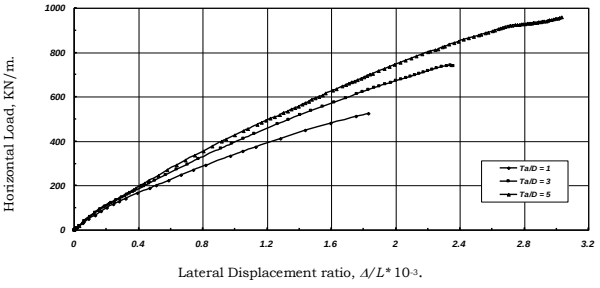

Fig. 3. Load-Displacement relationship at pile head due to various values of Anchor-Block Height ratio, T_a/D. (D=0.60 m, L/D=30, B_a/D=2, S/D=3, E_p/E_s=500, ϕ=30^o).

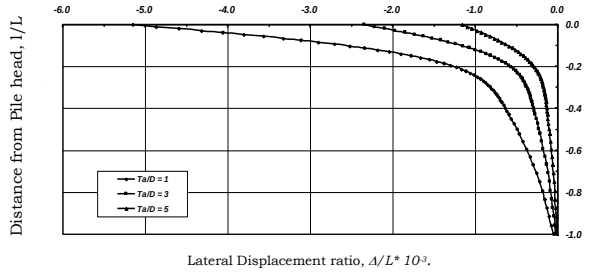

Fig. 4. Load-Displacement along pile length due to various values of Anchor-Block Height ratio, T_a/D. (D=0.60 m, L/D=30, B_a/D=2, S/D=3, E_p/E_s=500, ϕ=30^o).

5.2. Shearing force variation along the pile length

Fig. 5 shows the variation of shearing force, Q along the pile length due to different values of T_a/D ratio. It can be noted from the plot that the distribution of shearing force is concentrated within the top two fifths of the pile length and beyond that the shearing force could be zero for all analyzed modals. This may be attributed to the uniform of the soil properties. The maximum positive shearing force happened at the pile head while the maximum negative happened at a point very close, to be at the top one fifth of the pile length. The results show a reduction in both positive and negative shearing force. This reduction was 30 and 43% for positive shearing force and was 28 and 42% for negative shearing force as the T_a/D ratio increased from 1 to 3 and 5, respectively. This reduction could be attributed due to the contribution of passive earth pressure as mentioned above.

5.3. Bending moment variation along the pile length

Fig. 6 presents the distribution of bending moment, M along the pile length under different values of T_a/D ratio. The plots show that the maximum bending moments decreased with the increase of T_a/D ratio. For example, the reduction was about 14 and 21% as the T_a/D ratio increased from 1 to 3 and 5, respectively. The results show, also that the depth of maximum bending moment is observed to be at a point near to the top one tenth of the pile length. Moreover, the plots

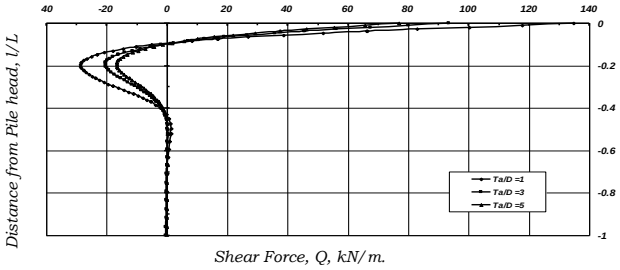

Fig. 5. Shear force distribution along pile length due to various values of Anchor-Block Height ratio, T_a/D. (D=0.60 m, L/D=30, B_a/D=2, S/D=3, E_p/E_s=500, ϕ=30°)

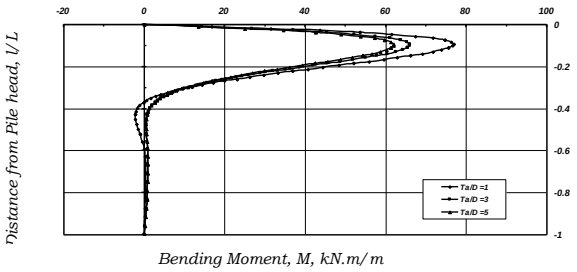

Fig. 6. Bending moment distribution along pile length due to various values of Anchor-Block Height ratio, T_a/D. (D=0.60 m, L/D=30, B_a/D=2, S/D=3, E_p/E_s=500, ϕ=30°).

show that the bending moment approximately developed within the top two fifth of the pile length and beyond this point the absolute value of the bending moment could be taken equal zero for all types of piles. This significant reduction could be attributed to uniform soil properties and the passive earth pressure developed over the anchored-block height as observed before.

6. Parametric study

In order to investigate the behavior of anchored-block pile system, the following parameters have been conducted:

1. Anchored-block thickness ratio, T_a/D;
2. Anchored-block width ratio, B_a/D;
3. Pile spacing ratio, S/D;
4. Pile length ratio, L/D;
5. Pile diameter, D;
6. Pile-soil stiffness ratio, E_p/E_s;
7. Angle of internal friction, ϕ;
8. Soil unit weight, γ,
9. Ground water level distance ratio, h_w/D;
10. Foundation level distance ratio, h_f/D; and,
11. Horizontal load, P_h.

6.1. Anchored-block thickness ratio, T_a/D as a variable

As mentioned before, anchored-block thickness ratio, T_a/D has a significant role in the response of the anchored-block pile structures. To determine this role, five values of this ratio have been adopted, (T_a/D = 1, 2, 3, 4 and 5). The other parameters of the model were considered constant as, D = 0.60 m., L/D = 30, B_a/D = 2, S/D = 3, ϕ=30°, γ_{dry} = 17

kN/m^3, P_h=*300* kN/m., and E_p/E_s = 500. The results obtained from different models showed that the lateral movements, the bending moments, the shearing forces developed over the pile shaft and the ultimate carrying load capacity of the system are considerably affected by the anchor-block thickness ratio, T_a/D.

6.1.1. Maximum lateral movement ratio, $(\Delta/L)_{mT}$

Fig. 7 represents the variation of the lateral movement ratio, $(\Delta/L)_{mT}$, due to different anchor-block thickness ratio, T_a/D. The results show a linear relationship on logarithmic scale. Based on the plotted results in Fig. 7, the maximum lateral movement ratio, $(\Delta/L)_{mT}$ developed at the pile head can be approximately expressed as:

$$\left(\frac{\Delta}{L}\right)_{mT} = \frac{17}{20E3}\left(\frac{T_a}{D}\right)^{-0.16} . \quad (3)$$

Where: $(\Delta/L)_{mT}$ is the maximum lateral movement ratio per meter due to different anchored-block thickness ratio, T_a/D.

6.1.2. Maximum shearing force, Q_{mT}

Fig. 8 illustrates the relationship between the maximum shearing force, Q_{mT} and the anchored-block thickness ratio, T_a/D.

The results show a linear trend on logarithmic scale. From the best fit of the plot in fig. 8, the maximum shearing force exerted on the pile shaft, Q_{mT} can be approximately obtained from:

$$Q_{mT} = \frac{73}{2}\left(\frac{T_a}{D}\right)^{-0.22} . \quad (4)$$

In which: Q_{mT} is the maximum shearing force

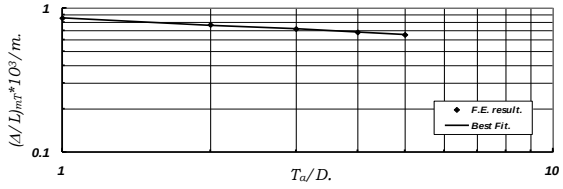

Fig. 7. Lateral Displacement ratio, $(\Delta/L)_{mT}$ versus Anchor-Block Height ratio, T_a/D. (D=0.60 m, L/D=30, B_a/D=2, S/D=3, E_p/E_s=500, ϕ=30°, P_h=300kN/m).

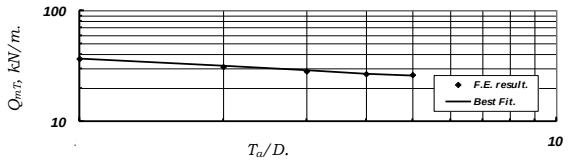

Fig. 8. Maximum shear force, Q_{mT} versus Anchor-Block Height ratio, T_a/D. (D=0.60 m, L/D=30, B_a/D=2, S/D=3, E_p/E_s=500, ϕ=30°, P_h=300kN/m).

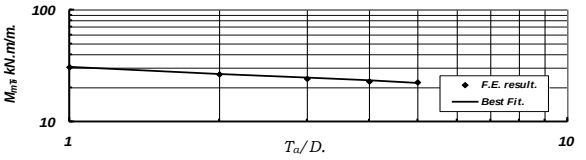

Fig. 9. Maximum bending moment, M_{mT} versus Anchor-Block *Height ratio*, T_a/D. (D=0.60 m, L/D=30, B_a/D=2, S/D=3, E_p/E_s=500, ϕ=30°, P_h=300kN/m).

in *kN/m.* due to different anchored-block thickness ratio, T_a/D.

6.1.3. Maximum bending moment, M_{mT}

The role of anchored-block thickness ratio, T_a/D, in the effect of the maximum bending moment, M_{mT} is presented in fig. 9. From the best fit of this plot, the maximum bending moment, M_{mT} may be approximately given by:

$$M_{mT} = \frac{153}{5}\left(\frac{T_a}{D}\right)^{-0.20} . \quad (5)$$

In which: M_{mT} is the maximum bending moment exerted in the pile shaft in *kN.m/m.* due to different anchored-block thickness ratio, T_a/D.

6.1.4. Ultimate lateral load, P_{UT}

Fig. 10 presents the relationship between the ultimate lateral load, P_{UT} and the anchored-block thickness ratio, T_a/D.

The results showed a linear relationship on semi-logarithmic scale. From the best fit of the plot in fig. 10, the ultimate lateral load, P_{UT} due to anchored-block thickness ratio, T_a/D may be given as:

$$P_{UT} = 457\, e^{0.155\left(\frac{T_a}{D}\right)} . \quad (6)$$

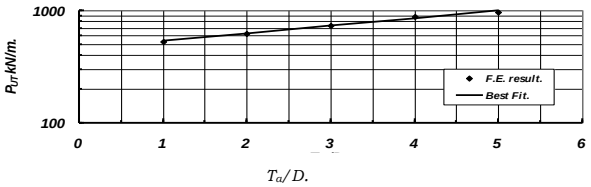

Fig. 10. Ultimate lateral load, P_{UT} versus Anchor-Block Height ratio, T_a/D. *(D=0.60 m, L/D=30, B_a/D=2, S/D=3, E_p/E_s=500, ϕ=30°, P_h=300*kN/m*).*

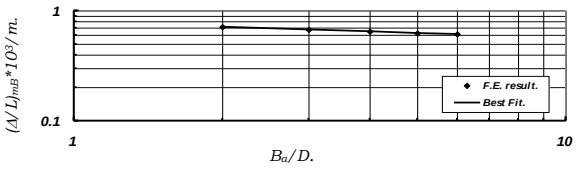

Fig. 11. Lateral Displacement ratio, $(\Delta/L)_{mB}$ versus Anchor-Block Width ratio, B_a/D. *(D=0.60 m, L/D=30, T_a/D=3, S/D=3, E_p/E_s=500, ϕ=30°, P_h=300*kN/m*).*

In which: P_{UT} is the ultimate lateral load in *kN/m.* due to different values of the anchored-block thickness ratio, T_a/D.

6.2. Anchored-block width ratio, B_a/D as a variable

Anchored-block width ratio, B_a/D has been found to have a little effect on the lateral displacement ratio, Δ/L but it has a great effect in shearing forces, Q and bending moments, M exerted along the pile shaft, in which B_a is the anchored-block width. Moreover, it affected significantly the load carrying capacity of the anchor-block pile system. To determine the effect of anchored-block width ratio, B_a/D, five values of this ratio have been considered, (B_a/D = 2, 3, 4, 5 and 6). The other parameters of the model were considered constant as, *D = 0.60 m., L/D = 30, T_a/D = 3, S/D = 3, ϕ=30°, γ_{dry} = 17 kN/m³, P_h=300 kN/m., and E_p/E_s = 500.* The results obtained from different models will be demonstrated in the following subsections.

6.2.1. Maximum lateral movement ratio, $(\Delta/L)_{mB}$

Fig. 11 illustrates the relationship between the lateral movement ratio, $(\Delta/L)_{mB}$ and the anchored-block width ratio, B_a/D.

The results show a linear relationship on logarithmic scale. Based on the best fit results in fig. 11, the maximum lateral movement ratio, $(\Delta/L)_{mB}$ developed at the pile head can be approximately expressed as:

$$\left(\frac{\Delta}{L}\right)_{mB} = \frac{19}{17}\left(\frac{\Delta}{L}\right)_{mT}\left(\frac{B_a}{D}\right)^{-0.14}. \qquad (7)$$

Where: $(\Delta/L)_{mB}$ is the maximum lateral movement ratio per meter due to different anchored-block width ratio, B_a/D.

6.2.2. Maximum shearing force, Q_{mB}

Fig. 12 presents the relationship between the maximum shearing force, Q_{mB} and the anchored-block width ratio, B_a/D. The results show a linear trend on semi-logarithmic scale. From the best fit of the plot in fig.12, the maximum shearing force exerted on the pile shaft, Q_{mB} can be approximately obtained from:

$$Q_{mB} = \frac{53}{25} Q_{mT}\, e^{-0.38\left(\frac{B_a}{D}\right)}. \qquad (8)$$

In which: Q_{mB} is the maximum shearing force in *kN/m.* due to different anchored-block width ratio, B_a/D.

6.2.3. Maximum bending moment, M_{mB}

The role of anchored-block width ratio, T_a/D, in the effect of the maximum bending moment, M_{mB} is illustrated in fig. 13. The results showed a linear relationship on semi-logarithmic scale. From the plots in fig. 13, the maximum bending moment, M_{mB} may be approximately given by:

$$M_{mB} = \frac{29}{20} M_{mT}\, e^{-0.18\left(\frac{B_a}{D}\right)}. \qquad (9)$$

In which: M_{mB} is the maximum bending moment exerted in the pile shaft in *kN.m/m.* due to different anchored-block width ratio, B_a/D.

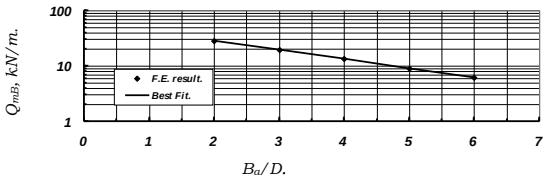

Fig. 12. Maximum shear force, Q_{mT} versus Anchor-Block Width ratio, B_a/D. (D=0.60 m, L/D=30, T_a/D=3, S/D=3, E_p/E_s=500, ϕ=30°, P_h=300kN/m).

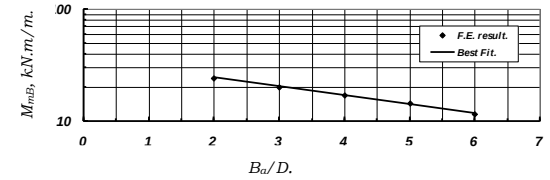

Fig. 13. Maximum bending moment, M_{mB} versus Anchor-Block Width ratio, B_a/D. (D=0.60 m, L/D=30, T_a/D=3, S/D=3, E_p/E_s=500, ϕ=30°, P_h=300kN/m).

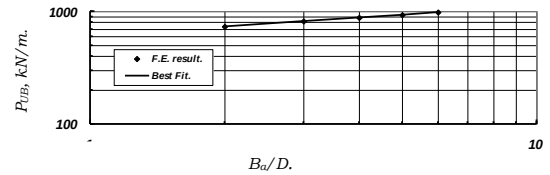

Fig. 14. Ultimate lateral load, P_{UB} versus Anchor-Block Width ratio, B_a/D. (D=0.60 m, L/D=30, T_a/D=3, S/D=3, E_p/E_s=500, ϕ=30°, P_h=300kN/m).

6.2.4. Ultimate lateral load, P_{UB}

Fig. 14 represents the variation of the ultimate lateral load, P_{UB} due to different anchored-block width ratio, B_a/D. The results showed a linear relationship on logarithmic scale. From the best fit of the plot in fig. 14, the ultimate lateral load, P_{UB} due to anchored-block width ratio, B_a/D may be given as:

$$P_{UB} = \frac{11}{13} P_{UT} \left(\frac{B_a}{D} \right)^{0.26} . \quad (10)$$

In which: P_{UB} is the ultimate lateral load in kN/m. due to different values of the anchored-block width ratio, B_a/D.

6.3. Pile spacing ratio, S/D as a variable

To determine the contribution of pile spacing ratio, S/D on the internal forces of the anchored-block pile system, five values of S/D ratio have been conducted, (S/D= 2, 3, 4, 5 and 6). The obtained results show a considerable effect of the pile spacing ratio, S/D linear relationship on the internal forces and the ultimate carrying load capacity of the structure. The internal forces along the pile shaft have been significantly reduced by reducing the pile spacing ratio, S/D. And, the ultimate carrying load of the structure has been increased with the reducing of S/D ratio. To define the contribution of the pile spacing ratio, S/D on the stability of the structure system, the following parameters D = 0.60 m., L/D = 30, T_a/D = 3, B_a/D = 2, ϕ=30°, γ_{dry} = 17 kN/m^3, P_h=300 kN/m., and E_p/E_s = 500 were considered constant. The results showed a linear trend as will be shown in the following subsections.

6.3.1. Maximum lateral movement ratio, $(\Delta/L)_{mS}$

Fig.15 illustrates the relationship between the lateral movement ratio, $(\Delta/L)_{mS}$ and the pile spacing ratio, S/D. The results show a linear relationship on logarithmic scale. Based on the best fit results in fig. 15, the maximum lateral movement ratio, $(\Delta/L)_{mS}$ developed at the pile head can be expressed as:

$$\left(\frac{\Delta}{L} \right)_{mS} = \frac{40}{47} \left(\frac{\Delta}{L} \right)_{mB} \left(\frac{S}{D} \right)^{0.17} . \quad (11)$$

Where: $(\Delta/L)_{mS}$ is the maximum lateral movement ratio per meter due to different pile spacing ratio, S/D.

6.3.2. Maximum shearing force, Q_{mS}

Fig. 16 presents the relationship between the maximum shearing force, Q_{mS} and the pile spacing ratio, S/D. The results show a linear

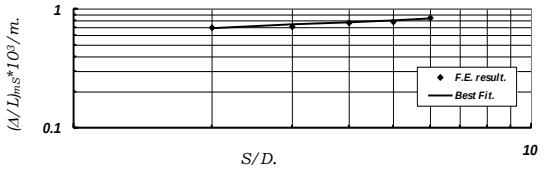

Fig. 15. Lateral Displacement ratio, $(\Delta/L)_{mS}$ versus Pile Spacing ratio, S/D. (D=0.60 m, L/D=30, T_a/D=3, B_a/D=2, E_p/E_s=500, ϕ=30°, P_h=300kN/m).

trend on semi-logarithmic scale. From the best fit of the plot in fig.1 6, the maximum shearing force exerted on the pile shaft, Q_{mS} can be obtained from:

$$Q_{mS} = \frac{49}{20} Q_{mB} e^{-0.30\left(\frac{S}{D}\right)}. \quad (12)$$

In which: Q_{mS} is the maximum shearing force in *kN/m.* due to different pile spacing ratio, *S/D.*

6.3.3. Maximum bending moment, M_{mS}

The role of pile spacing ratio, *S/D*, in the effect of the maximum bending moment, M_{mS} is illustrated in fig. 17. The results showed a linear relationship on semi-logarithmic scale. From the plots in fig. 17, the maximum bending moment, M_{mS} may be given by:

$$M_{mS} = \frac{44}{15} M_{mB} e^{-0.35\left(\frac{S}{D}\right)}. \quad (13)$$

In which: M_{mS} is the maximum bending moment exerted in the pile shaft in *kN.m/m.* due to different pile spacing ratio, *S/D.*

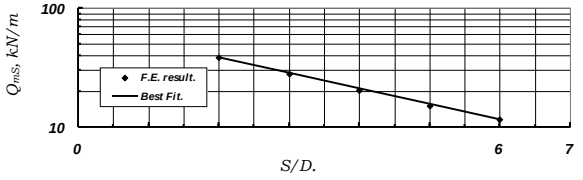

Fig. 16. Maximum shear force, Q_{mS} versus Pile Spacing ratio, *S/D. (D*=0.60 m, *L/D*=30, T_a/D=3, B_a/D=2, E_p/E_s=500, ϕ=30°, P_h=*300*kN/m*).*

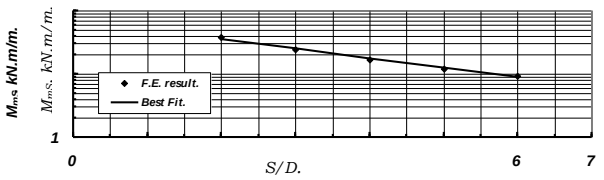

Fig. 17. Maximum bending moment, M_{mS} versus Pile Spacing ratio, *S/D. (D*=0.60 m, *L/D*=30, T_a/D=3, B_a/D=2, E_p/E_s=500, ϕ=30°, P_h=300kN/m*).*

6.3.4. Ultimate lateral load, P_{US}

Fig. 18 represents the variation of the ultimate lateral load, P_{US} due to different pile spacing ratio, *S/D.* The results showed a linear relationship on logarithmic scale. From the best fit of the plot in fig. 18, the ultimate lateral load, P_{US} due to pile spacing ratio, *S/D* may be given as:

$$P_{US} = \frac{33}{25} P_{UB} e^{-0.08\left(\frac{S}{D}\right)}. \quad (14)$$

In which: P_{US} is the ultimate lateral load in *kN*/m. due to different values of the pile spacing ratio, *S/D.*

6.4. Pile length ratio, L/D as a variable

To represent the behavior of the anchored-block pile system due to the change of the pile length ratio, *L/D*, six values of *L/D* ratio have been adopted, (*L/D*= 15, 20, 25, 30, 35 and 40). The other parameters were considered constant as, *(D = 0.60 m., S/D = 3, T_a/D = 3, B_a/D = 2, ϕ=30°, γ_{dry} = 17 kN/m³, P_h=300 kN/m., and E_p/E_s = 500).* The results showed a considerable effect of the pile length ratio, *S/D* on the internal forces and the ultimate carrying load capacity of the structure. The maximum lateral movement ratio, $(\Delta/L)_m$ has been greatly reduced as the *L/D* ratio increased. Both the maximum shearing force, Q_m and the maximum bending moment, M_m exerted along the pile shaft have been reduced by increasing the pile length ratio, *L/D.* Moreover, the ultimate carrying load capacity of the system has been significantly increased with the increasing of the *L/D* ratio. The results showed a linear trend in semi-logarithmic scale as will be shown in the following subsections.

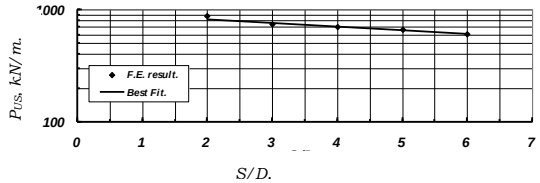

Fig. 18. Ultimate lateral load, P_{US} versus Pile Spacing ratio, *S/D. (D*=0.60 m, *L/D*=30, T_a/D=3, B_a/D=*2,* E_p/E_s=500, ϕ=30°, P_h=300kN/m*).*

6.4.1. Maximum lateral movement ratio, $(\Delta/L)_{Ml}$

Fig. 19 illustrates the variation between the lateral movement ratio, $(\Delta/L)_{mL}$ and the pile length ratio, L/D.

The results show a linear relationship on semi-logarithmic scale. Based on the plots in fig. 19, the maximum lateral movement ratio, $(\Delta/L)_{mL}$ exerted at the pile head may be given from:

$$\left(\frac{\Delta}{L}\right)_{mL} = \frac{35}{4}\left(\frac{\Delta}{L}\right)_{mS} e^{-0.07\left(\frac{L}{D}\right)}. \quad (15)$$

Where: $(\Delta/L)_{mL}$ is the maximum lateral movement ratio per meter due to different pile length ratio, L/D.

6.4.2. Maximum shearing force, Q_{mL}

Fig. 20 illustrates the relationship between the maximum shearing force, Q_{mL} and different values of the pile length ratio, L/D. The results show a linear trend on semi-logarithmic scale. From the best fit plots in this figure, the maximum shearing force exerted along the pile shaft, Q_{mL} may be expressed as:

$$Q_{mL} = \frac{6}{5} Q_{mS} e^{-0.006\left(\frac{L}{D}\right)}. \quad (16)$$

In which: Q_{mL} is the maximum shearing force in kN/m. due to different pile length ratio, L/D.

6.4.3. Maximum bending moment, M_{mL}

The effect of pile length ratio, L/D, in the maximum bending moment, M_{mL} exerted along the pile shaft is illustrated in fig. 21. The

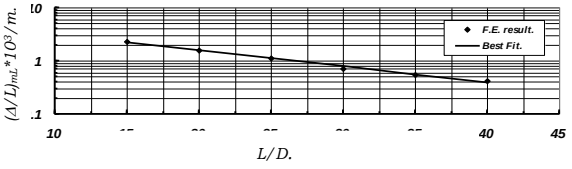

Fig. 19. Lateral Displacement ratio, $(\Delta/L)_{mL}$ versus Pile Length ratio, L/D. (D=0.60 m, S/D=3, T_a/D=3, B_a/D=2, E_p/E_s=500, ϕ=30°, P_h=300kN/m).

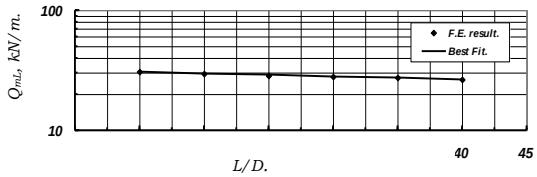

Fig. 20. Maximum shear force, Q_{mL} versus Pile Length ratio, L/D. (D=0.60 m, S/D=3, T_a/D=3, B_a/D=2, E_p/E_s=500, ϕ=30°, P_h=300kN/m).

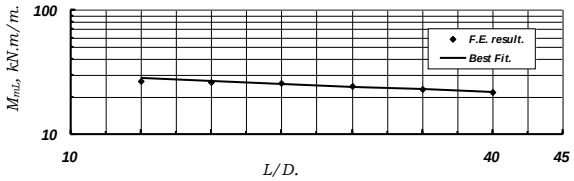

Fig. 21. Maximum bending moment, M_{mL} versus Pile Length ratio, L/D. (D=0.60 m, S/D=3, T_a/D=3, B_a/D=2, E_p/E_s=500, ϕ=30°, P_h=300kN/m).

results showed a linear relationship on semi-logarithmic scale. From the plots in fig. 21, the maximum bending moment, M_{mL} may be given by:

$$M_{mL} = \frac{13}{10} M_{mS} e^{-0.01\left(\frac{L}{D}\right)}. \quad (17)$$

In which: M_{mL} is the maximum bending moment exerted in the pile shaft in $kN.m/m$. due to different pile length ratio, L/D.

6.4.4. Ultimate lateral load, P_{UL}

Fig. 22 represents the relationship between the ultimate lateral load, P_{UL} and different values of pile length ratio, L/D. The results showed a linear relationship on semi-logarithmic scale. From the best fit of the plot in fig. 22, the ultimate lateral load, P_{UL} due to pile length ratio, L/D may be expressed as:

$$P_{UL} = \frac{19}{26} P_{US} e^{0.01\left(\frac{L}{D}\right)}. \quad (18)$$

In which: P_{UL} is the ultimate lateral load in kN/m. due to different values of the pile length ratio, L/D.

6.5. Pile diameter, d as a variable

Results obtained from different models have shown that pile diameter had a great effect on the behavior of the anchored-block pile system. The maximum lateral movement ratio, $(\Delta/L)_m$ has been greatly reduced as the pile diameter, D increased. The maximum shearing force, Q_m, the maximum bending moment, M_m and the ultimate carrying load capacity of the system has been significantly increased as the pile diameter, D increased. In this work, four values of pile diameter, D have been adopted, (D= *0.40, 0.60, 0.80* and *1.00 m.*). The other parameters were considered constant as, $(L/D = 30, S/D = 3, T_a/D = 3, B_a/D = 2, \phi=30^o, \gamma_{dry} = 17\ kN/m^3, P_h=300\ kN/m.,$ *and* $E_p/E_s = 500)$. The following subsections present the results obtained from different pile diameter, D models.

6.5.1. Maximum lateral movement ratio, $(\Delta/L)_{mD}$

Fig. 23 illustrates the variation between the lateral movement ratio, $(\Delta/L)_{mD}$ and different pile diameter, D.

The results show a linear relationship on logarithmic scale. Based on the plots in fig. 23, the maximum lateral movement ratio, $(\Delta/L)_{mD}$ exerted at the pile head may be approximately given from:

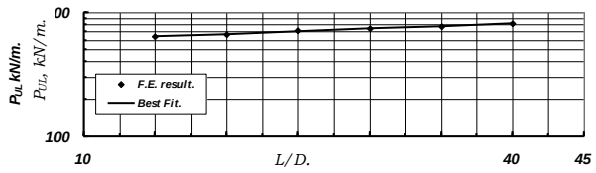

Fig. 22. Ultimate lateral load, P_{UL} versus Pile Length ratio, L/D. (D=0.60 m, S/D=3, T_a/D=3, B_a/D=2, E_p/E_s=500, ϕ=30°, P_h=300kN/m).

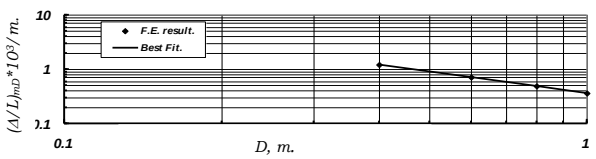

Fig. 23. Lateral Displacement ratio, $(\Delta/L)_{mD}$ versus Pile Diameter, D. (L/D=30, S/D=3, T_a/D=3, B_a/D=2, E_p/E_s=500, ϕ=30°, P_h=300kN/m).

$$\left(\frac{\Delta}{L}\right)_{mD} = \frac{13}{28}\left(\frac{\Delta}{L}\right)_{mL} D^{-1.30}. \quad (19)$$

Where: $(\Delta/L)_{mD}$ is the maximum lateral movement ratio per meter due to different pile diameter, D.

6.5.2. Maximum shearing force, Q_{mD}

Fig. 24 illustrates the relationship between the maximum shearing force, Q_{mD} and different values of the pile diameter, D. The results show a linear trend on logarithmic scale. From the best fit plots in this figure, the maximum shearing force exerted along the pile shaft, Q_{mD} may be expressed as:

$$Q_{mD} = \frac{13}{10} Q_{mL} D^{0.50}. \quad (20)$$

In which: Q_{mD} is the maximum shearing force in *kN/m.* due to different pile diameter, D.

6.5.3. Maximum bending moment, M_{mD}

The effect of pile diameter, D, in the maximum bending moment, M_{mD} exerted along the pile shaft is illustrated in fig. 25. The results showed a linear relationship on logarithmic scale. From the plots in fig. 25, the maximum bending moment, M_{mD} may be approximately given by:

$$M_{mD} = \frac{49}{25} M_{mL} D^{1.30}. \quad (21)$$

In which: M_{mD} is the maximum bending moment exerted in the pile shaft in *kN.m/m.* due to pile diameter, D.

6.5.4. Ultimate lateral load, P_{UD}

Fig. 26 represents the relationship between the ultimate lateral load, P_{UD} and

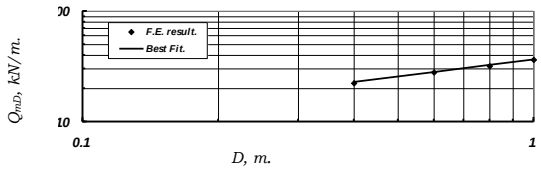

Fig. 24. Maximum shear force, Q_{mD} versus Pile Diameter, D. (L/D=30, S/D=3, T_a/D=3, B_a/D=2, E_p/E_s=500, ϕ=30°, P_h=300kN/m).

different values of pile diameter, *D*. The results showed a linear relationship on semi-logarithmic scale. From the best fit of the plot in fig. 26, the ultimate lateral load, P_{UD} due to pile diameter, *D* may be expressed as:

$$P_{UD} = \frac{63}{100} P_{UL}\, e^{0.8D}. \quad (22)$$

In which: P_{UD} is the ultimate lateral load in *kN*/m. due to different values of the pile diameter, *D*.

6.6. pile-soil stiffness ratio, E_p/E_s as a variable

To obtain the contribution of pile-stiffness ratio, E_p/E_s on the stability of the anchored-block pile system, seven values of E_p/E_s ratio, which ranged from low to high stiffness sand, have been adopted, (E_p/E_s = 1000, 666, 500, 400, 333, 286 and 250). The other parameters were considered constant as, *(D = 0.60 m., L/D = 30, S/D = 3, T_a/D = 3, B_a/D = 2, ϕ=30°, γ_{dry} = 17 kN/m³, P_h=300 kN/m., and E_p =20*10⁶ kN/m²).* Results from different models have shown a significant contribution of the pile-stiffness ratio, E_p/E_s on the behavior of the anchored-block pile system. The lateral movement, the shearing force and the bending moment and the ultimate load carrying capacity of the system have been

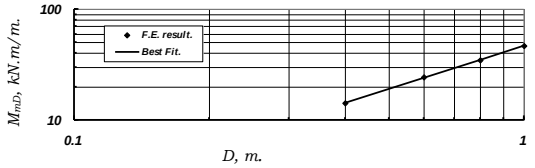

Fig. 25. Maximum bending moment, M_{mD} versus Pile Diameter, *D*. (L/D=30, S/D=3, T_a/D=3, B_a/D=2, E_p/E_s=500, ϕ=30°, P_h=300kN/m).

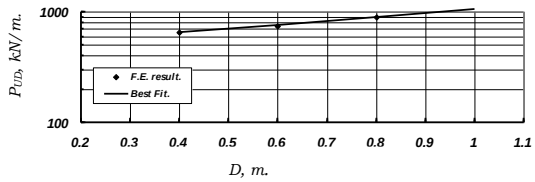

Fig. 26. Ultimate lateral load, P_{UD} versus Pile Diameter, D. (L/D=30, S/D=3, T_a/D=3, B_a/D=2, E_p/E_s=500, ϕ=30°, P_h=300kN/m).

significantly reduced as the pile-stiffness ratio, E_p/E_s reduced. The results showed a linear trend on logarithmic scale. The following subsections present the results obtained from different pile-stiffness ratio, E_p/E_s models.

6.6.1. Maximum lateral movement ratio, $(\Delta/L)_{mE}$

Based on the obtained results, the maximum lateral movement ratio, $(\Delta/L)_{mE}$ exerted at the pile head may be approximately given from:

$$\left(\frac{\Delta}{L}\right)_{mE} = \frac{1}{406}\left(\frac{\Delta}{L}\right)_{mD}\left(\frac{E_p}{E_s}\right)^{0.97}. \quad (23)$$

Where: $(\Delta/L)_{mE}$ is the maximum lateral movement ratio per meter due to different pile-stiffness ratio, E_p/E_s.

6.6.2. Maximum shearing force, Q_{mE}

From the best fit of the results, the maximum shearing force exerted along the pile shaft, Q_{mE} may be expressed as:

$$Q_{mE} = \frac{29}{250} Q_{mD}\left(\frac{E_p}{E_s}\right)^{0.35}. \quad (24)$$

In which: Q_{mE} is the maximum shearing force in *kN/m.* due to different pile-stiffness ratio, E_p/E_s.

6.6.3. Maximum bending moment, M_{mE}

The maximum bending moment, M_{mE} due to different values of pile-stiffness ratio, E_p/E_s may be approximately given by:

$$M_{mE} = \frac{1}{25} M_{mD}\left(\frac{E_p}{E_s}\right)^{0.52}. \quad (25)$$

In which: M_{mE} is the maximum bending moment exerted in the pile shaft in *kN.m/m.* due to different pile-stiffness ratio, E_p/E_s.

6.6.4. Ultimate lateral load, P_{UE}

Moreover, the ultimate lateral load, P_{UE} due to pile-stiffness ratio, E_p/E_s may be expressed as:

$$P_{UE} = \frac{2}{3} P_{UL} \left(\frac{E_p}{E_s} \right)^{0.06} . \quad (26)$$

In which: P_{UE} is the ultimate lateral load in *kN*/m. due to different values of the pile-stiffness ratio, E_p/E_s.

6.7. Angle of internal friction, ϕ as a variable

Angle of internal friction, ϕ is one of the most affecting factors in the analysis of the anchored-block pile system. Both the internal forces and lateral displacements have been considerably reduced as angle of internal friction, ϕ increased. Also, the ultimate load carrying capacity of the system has been significantly increased as the angle of internal friction, ϕ increased.

To determine the contribution of angle of internal friction, ϕ, five values of the angle of internal friction, ϕ, which ranged to represent loose, medium and dense sand, have been adopted, *(ϕ = 25, 30, 35, 40 and 45^o).* The other parameters were considered constant as, *(D = 0.60 m., L/D = 30, S/D = 3, T_a/D = 3, B_a/D = 2, E_p/E_s =500, γ_{dry} = 17 kN/m^3, P_h=300 kN/m., and E_p =20*10^6 kN/m^2).* Results from different models have shown a linear trend on semi-logarithmic scale. The following subsections present the results obtained from models of different angle of internal friction, ϕ.

6.7.1. Maximum lateral movement ratio, $(\Delta/L)_{m\phi}$

Based on the obtained results, the maximum lateral movement ratio, $(\Delta/L)_{m\phi}$ exerted at the pile head may be approximately given from:

$$\left(\frac{\Delta}{L} \right)_{m\phi} = 5 \left(\frac{\Delta}{L} \right)_{mE} e^{-0.05\phi} . \quad (27)$$

Where: $(\Delta/L)_{m\phi}$ is the maximum lateral movement ratio per meter due to different angle of internal friction, ϕ.

6.7.2. Maximum shearing force, $Q_{m\phi}$

From the best fit of the results, the maximum shearing force exerted along the pile shaft, $Q_{m\phi}$ may be expressed as:

$$Q_{m\phi} = \frac{11}{5} Q_{mE} e^{-0.025\phi} . \quad (28)$$

In which: $Q_{m\phi}$ is the maximum shearing force in *kN/m.* due to different angle of internal friction, ϕ.

6.7.3. Maximum bending moment, $M_{m\phi}$

The maximum bending moment, $M_{m\phi}$ due to different values of angle of internal friction, ϕ may be approximately given by:

$$M_{m\phi} = \frac{37}{20} M_{mE} e^{-0.02\phi} . \quad (29)$$

In which: $M_{m\phi}$ is the maximum bending moment exerted in the pile shaft in *kN.m/m.* due to angle of internal friction, ϕ.

6.7.4. Ultimate lateral load, $P_{U\phi}$

The ultimate lateral load, $P_{U\phi}$ due to angle of internal friction, ϕ may be expressed as:

$$P_{U\phi} = \frac{51}{125} P_{UE} e^{0.03\phi} . \quad (30)$$

In which: $P_{U\phi}$ is the ultimate lateral load in *kN*/m. due to different values of angle of internal friction, ϕ.

6.8. Soil unit weight, γ as a variable

To obtain the contribution of angle of soil unit weight, γ on the analysis of the anchored-block pile system, six values of the soil unit weight, γ have been adopted, *(γ= 15, 16, 17, 18, 19 and 20 kN/m^3).* The other parameters were considered constant as, *(D = 0.60 m., L/D = 30, S/D = 3, T_a/D = 3, B_a/D = 2, E_p/E_s=500, ϕ = 30^o, P_h=300 kN/m., and E_p =20*10^6 kN/m^2).* Results from different models showed a considerable reduction in the internal forces and lateral displacement as the soil unit weight, γ increased. In addition, the ultimate load carrying capacity of the system has been significantly increased as the soil unit weight, γ increased. The results also showed a linear trend on semi-logarithmic scale. Results obtained from models of different soil unit

weight, γ will be presented in the following subsections.

6.8.1. Maximum Lateral Movement ratio, $(\Delta/L)_{m\gamma}$

Based on the obtained results, the maximum lateral movement ratio, $(\Delta/L)_{m\gamma}$ exerted at the pile head may be approximately given from:

$$\left(\frac{\Delta}{L}\right)_{m\gamma} = \frac{21}{10}\left(\frac{\Delta}{L}\right)_{m\phi} e^{-0.05\gamma}. \quad (31)$$

Where: $(\Delta/L)_{m\gamma}$ is the maximum lateral movement ratio per meter due to different soil unit weight, γ.

6.8.2. Maximum shearing force, $Q_{m\gamma}$

From the best fit of the results, the maximum shearing force exerted along the pile shaft, $Q_{m\gamma}$ may be expressed as:

$$Q_{m\gamma} = \frac{5}{2} Q_{m\phi}\, e^{-0.055\gamma}. \quad (32)$$

In which: $Q_{m\gamma}$ is the maximum shearing force in *kN/m.* due to different angle of internal friction, ϕ.

6.8.3. Maximum bending moment, $M_{m\gamma}$

The maximum bending moment, $M_{m\gamma}$ due to different values of soil unit weight, γ may be approximately given by:

$$M_{m\gamma} = 2.00\, M_{m\phi}\, e^{-0.04\gamma}. \quad (33)$$

In which: $M_{m\gamma}$ is the maximum bending moment exerted in the pile shaft in *kN.m/m.* due to soil unit weight, γ.

6.8.4. Ultimate lateral load, $P_{U\gamma}$

The ultimate lateral load, $P_{U\gamma}$ due to soil unit weight, γ may be expressed as:

$$P_{U\gamma} = \frac{2}{5} P_{U\phi}\, e^{0.054\gamma}. \quad (34)$$

In which: $P_{U\gamma}$ is the ultimate lateral load in *kN*/m. due to different values of soil unit weight, γ.

6.9. Ground water level distance ratio, h_w/D as a variable

Results obtained from models of different ground water level distance ratios, h_w/D have shown that h_w/D ratio had a considerable effect on the behavior of the anchored-block pile system, in which h_w is the distance from the ground to the ground water level. The maximum lateral movement ratio, $(\Delta/L)_m$, the maximum shearing force, Q_m, and the maximum bending moment, M_m has been reduced as the ratio h_w/D increased. Also, the ultimate carrying load capacity of the anchored-block pile system has been increased as the ground water level distance ratio, h_w/D increased. In the present work, seven values of the h_w have been considered, *(h_w = 0.0, 1.0, 2.0, 3.0, 4.0, 5.0 and 6.0 m.).* The other parameters were considered constant as, *(D = 0.60 m, L/D = 30, S/D = 3, T_a/D = 3, B_a/D = 2, ϕ=30°, γ_{dry} = 17 kN/m^3, P_h=300 kN/m., and E_p/E_s = 500).* The following subsections present the results obtained from different ground water level distance ratios, h_w/D models.

6.9.1. Maximum lateral movement ratio, $(\Delta/L)_{mw}$

Based on the obtained results, the maximum lateral movement ratio, $(\Delta/L)_{mw}$ exerted at the pile head may be approximately given from:

$$\left(\frac{\Delta}{L}\right)_{mw} = \frac{11}{10}\left(\frac{\Delta}{L}\right)_{m\gamma} e^{-0.001\left(\frac{h_w}{D}\right)}. \quad (35)$$

Where: $(\Delta/L)_{mw}$ is the maximum lateral movement ratio per meter due to different ground water level distance ratios, h_w/D.

6.9.2. Maximum shearing force, Q_{mw}

From the best fit of the results, the maximum shearing force exerted along the pile shaft, Q_{mw} may be expressed as:

$$Q_{mw} = \frac{11}{5} Q_{m\gamma}\, e^{-0.02\left(\frac{h_w}{D}\right)}. \quad (36)$$

In which: Q_{mw} is the maximum shearing force in *kN/m.* due to different ground water level distance ratios, h_w/D.

6.9.3. Maximum bending moment, M_{mw}

The maximum bending moment, M_{mw} due to different values of ground water level distance ratios, h_w/D may be approximately given by:

$$M_{mw} = \frac{53}{50} M_{m\gamma}\, e^{-0.01\left(\frac{h_w}{D}\right)}. \quad (37)$$

In which: M_{mw} is the maximum bending moment exerted in the pile shaft in *kN.m/m.* due to different ground water level distance ratios, h_w/D.

6.9.4. Ultimate lateral load, P_{Uw}

As well as, the ultimate lateral load, P_{Uw} due to different ground water level distance ratios, h_w/D may be expressed as:

$$P_{Uw} = \frac{37}{50} P_{U\gamma}\, e^{0.036\left(\frac{h_w}{D}\right)}. \quad (38)$$

In which: P_{Uw} is the ultimate lateral load in *kN*/m. due to different values of different ground water level distance ratios, h_w/D.

6.10. Foundation level distance ratio, h_f/D as a variable

Foundation level distance ratio, h_f/D is one of the most affecting factors in the analysis of the anchored-block pile system, and in which h_f is the distance from the ground to the foundation level. Both the internal forces and lateral displacements have been considerably reduced as foundation level distance ratio, h_f/D increased. The ultimate load carrying capacity of the system has been significantly increased as the h_f/D ratio increased.

To determine the contribution of the foundation level distance ratio, h_f/D, five values of the h_f have been adopted, *(h_f =3.0, 4.0, 5.0, 6.0 and 7.0 m.).* The other parameters were considered constant as, *(D = 0.60 m., L/D = 30, S/D = 3, T_a/D = 3, B_a/D = 2, E_p/E_s=500, ϕ = 30°, γ_{dry} = 17 kN/m^3, P_h=300 kN/m., and E_p =20*10^6 kN/m^2).* Results from different models have shown a linear trend on semi-logarithmic scale. The following subsections present the results obtained from models of different foundation level distance ratio, h_f/D.

6.10.1. Maximum lateral movement ratio, $(\Delta/L)_{mf}$

Based on the obtained results, the maximum lateral movement ratio, $(\Delta/L)_{mf}$ exerted at the pile head may be approximately given from:

$$\left(\frac{\Delta}{L}\right)_{mf} = 2\left(\frac{\Delta}{L}\right)_{mw} e^{-0.08\left(\frac{h_f}{D}\right)}. \quad (39)$$

Where: $(\Delta/L)_{mf}$ is the maximum lateral movement ratio per meter due to different values of foundation level distance ratio, h_f/D.

6.10.2. Maximum shearing force, Q_{mf}

From the best fit of the results, the maximum shearing force exerted along the pile shaft, Q_{mf} may be expressed as:

$$Q_{mf} = \frac{23}{10} Q_{mw}\, e^{-0.11\left(\frac{h_f}{D}\right)}. \quad (40)$$

In which: Q_{mf} is the maximum shearing force in *kN/m.* due to different values of foundation level distance ratio, h_f/D.

6.10.3. Maximum bending moment, M_{mf}

The maximum bending moment, M_{mf} due to different values of foundation level distance ratio, h_f/D may be approximately given by:

$$M_{mf} = \frac{23}{10} M_{mw}\, e^{-0.10\left(\frac{h_f}{D}\right)}. \quad (41)$$

In which: M_{mf} is the maximum bending moment exerted in the pile shaft in *kN.m/m.* due to different values of foundation level distance ratio, h_f/D.

6.10.4. Ultimate lateral load, P_{ult}

The ultimate lateral load, P_{ult} due to different parameters pertaining to the anchored-block pile system may be expressed as:

$$P_{ult} = \frac{32}{125} P_{Uw}\, e^{0.165\left(\frac{h_f}{D}\right)}. \quad (42)$$

In which: P_{ult} is the ultimate lateral load in *kN*/m. due to different parameters pertaining to the anchored-block pile system.

6.11. Horizontal load, P_h as a variable

To obtain the effect of horizontal load, P_h on the design of the anchored-block pile system, seven values of the horizontal load, P_h have been adopted, *(P_h = 100, 200, 300, 400, 500, 600 and 700 kN/m)*. The other parameters were considered constant as, *(D = 0.60 m., L/D = 30, S/D = 3, T_a/D = 3, B_a/D = 2, E_p/E_s=500, ϕ = 30°, γ_{dry} = 17 kN/m^3, and E_p =20*10^6 kN/m^2).* The maximum lateral movement ratio, $(\Delta/L)_{max}$, the maximum shearing force, Q_{max}, the maximum bending moment, M_{max} and the ultimate load carried by the system, P_{ult} showed a linear trend on semi-logarithmic scale when the horizontal load, P_h plotted against them. The following subsections represent the results obtained from models loaded with different values of horizontal load, P_h.

6.11.1. Maximum lateral movement ratio, $(\Delta/L)_{max}$

Based on the obtained results, the maximum lateral movement ratio, $(\Delta/L)_{max}$ exerted at the pile head may be approximately given from:

$$\left(\frac{\Delta}{L}\right)_{max} = \frac{25}{37\,E3}\left(\frac{\Delta}{L}\right)_{mf} P_h^{1.27}. \qquad (43)$$

Where: $(\Delta/L)_{max}$ is the maximum lateral movement ratio per meter due to different values of horizontal load, P_h.

6.11.2. Maximum shearing force, Q_{max}

From the best fit of the results, the maximum shearing force exerted along the pile shaft, Q_{max} may be expressed as:

$$Q_{max} = \frac{1}{5500} Q_{mf}\, P_h^{1.50}. \qquad (44)$$

In which: Q_{max} is the maximum shearing force in *kN/m.* due to different parameters pertaining to the anchored-block pile system.

6.11.3. Maximum bending moment, M_{max}

The maximum bending moment, M_{max} due to different parameters pertaining to the anchored-block pile system may be approximately given by:

$$M_{max} = \frac{1}{1150} M_{mf}\, P_h^{1.23}. \qquad (45)$$

In which: M_{max} is the maximum bending moment exerted in the pile shaft in *kN.m/m.* due to different parameters pertaining to the anchored-block pile system.

7. Conclusions

Based on the results of this study, it may be concluded that all the parameters pertaining to the anchored-block pile system have a significant role on the performance of the system. The results presented show that the ultimate load carrying capacity of the system has been found to improve with increasing the parameters of the system. The maximum lateral movement at the pile head has been considerably reduced by increasing the pertaining parameters of the system. The maximum shearing force and the maximum bending moment exerted along the pile shaft has been also reduced. Results also show that the maximum positive shearing force occurred at the pile head while the maximum negative shearing force happened at a point very close, to be at the top one fifth of the pile head. Furthermore, the position of the maximum bending moment has been observed at a point near the top one tenth of the pile length. Formulas to evaluate the maximum lateral movement, shearing force and bending moment due to different design parameters of the anchored-block pile system are estimated and presented.

Notations

D	is the pile diameter,
Q	is the shearing force,
L	is the pile length,
M	is the bending moment,
S	is the Pile spacing,
f_s	is the side shear resistance of pile per unit length,

h_f is the distance from ground to the foundation level,
h_w is the distance from ground to the ground water level,
f_{eq} is the equivalent side shear resistance,
A_p is the area of pile cross section,
A_s is the surface area of pile per unit length,
B_a is the Anchored-block
E_p is the modulus of elasticity of pile,
E_s is the modulus of elasticity of soil,
L_a is the length of anchor block (in plan),
N_i is the number of piles in row i,
P_h is the horizontal load,
T_a is the thickness of anchored-block,
E_{eq} is the equivalent pile Young's modulus,
Q_{max} is the maximum shearing force,
M_{max} is the maximum bending moment,
P_{ult} is the ultimate lateral load,
Δ is the lateral displacement,
ϕ is the angle of internal friction,
ν_p is the Poisson's ratio of pile,
ν_s is the Poisson's ratio of soil,
γ_{pd} is the dry unit weight of pile,
γ_{sd} is the dry unit weight, and
$(\Delta/L)_{max}$ is the maximum lateral movement ratio.

References

[1] J.E. Bowles, Foundation Analysis and Design, Fifth Edition, McGraw-Hill Book Co., NY, New York (1996).

[2] H. Matlock, "Correlations for Design of Laterally Loaded Piles in Soft Clay", Proceedings of the Offshore Technology Conf., (1204), pp. 577-594 (1970).

[3] L.C. Reese, W.R. Cox, and F.D. Koop, "Field Testing and Analysis of Laterally Loaded Piles in Stiff Clay", Proceedings of the 7th Offshore Technology Conf., Vol. II (2312), pp. 671-690 (1975).

[4] L.C. Reese, and R.C. Welch, "Lateral Loading of Deep Foundations in Stiff Clay", Journal of Geotechnical Engineering Div., ASCE, Vol. 101 (GT7), pp. 633-649 (1975).

[5] F. Baguelin, R. Frank, and Y.M. Said, "Theoretical Study of Lateral Reaction Mechanism of Piles", Geotechnique, Vol. 27 (3), pp. 405-434 (1997).

[6] Y.K. Chow, "Axial and Lateral Response of Pile Groups Embedded in Non-Homogeneous Soils". International Journal for Numerical and Analytical Methods in Geomechanics, Vol. 11, pp. 621-638 (1987).

[7] S. Kumar, and L. Lalvani, "Lateral Load-Deflection Response of Drilled Shafts in Sand," International Engineering Journal-CV, Vol. 84, pp. 282-286 (2004).

[8] W.D. Guo, "On Critical Depth and Lateral Pile Response," Journal of Geotechnical and Geoenvironmental Engineering, ASCE, 11 (2002).

[9] W.D. Guo, "A Simplified approach for piles due to soil movement," Proceedings of 12th Pan-American Conference on Soil Mechanics and Geotechnical Engineering, Cambridge, MIT, U.S.A., Vol. 2, pp. 2215-2220 (2003).

[10] W.D. Guo, and B.T. Zhu, "Laterally loaded Fixed-Head piles in Sand", Proceedings of 9th Australia New Zeland Conference on Geomechanics, Auckland, New Zeland (2003).

[11] M. Alizadeh, L. and Lalvani, "Lateral Load-Deflection Response of Single Piles in Sand", Electronic Journal of Geotechnical Engineering, Vol. 5 (2000).

[12] R.L. Mokwa, J.M. and Duncan, "Experimental Evaluation of Lateral-Load Resistance of Pile Caps", Journal of Geotechnical and Geoenviornmental Engineering, Vol. 127 (2), pp. 185-192 (2001).

[13] D.K. Maharaj, "Load-Deflection Response of Laterally loaded Single Pile by Nonlinear Finite Element Analysis", Electronic Journal of Geotechnical Engineering, Vol. 7 (2002).

[14] P.A.Vermeer, and R.B.J. Brinkgreve, PLAXIS user's Manual, Version 6.1, Balkema, Rotterdam, Netherlands (1995).

[15] J.C. Nagtegaal, D.M. Parks, J.R. and Rice, "On Numerically Accurate Finite Element Solution in Fully Plastic Range", Comp. Math. Appl. Mech. Eng., Vol. 4 pp. 153-177 (1974).

[16] S.W. Sloan, and M.F. Randolph, "Numerical Prediction of Collapse loads using Finite Element Methods", International Journal of Numerical and Analytical Mathematics in Geomechanical Engineering, Vol. 6, pp. 47-76 (1982).

[17] C.S. Desai, L.D. Johnson, and C.M. Hargett, "Analysis of Pile-Supported Gravity Lock", Journal of Geotechnical Engineering, ASCE, Vol. 100 (9), pp. 1009-1029 (1974).

[18] P.A. Parakosa, and F.H. Kulhawy, "Piled Raft Foundation Design", Journal of Geotechnical and Geoenvironmental Engineering, ASCE, Vol. 127 (1), pp. 17-24 (2001).

Received June 11, 2005
Accepted September 13, 2005